Engineering Analysis with Boundary Elements 54 (2015) 86–96

Contents lists available at ScienceDirect

Engineering Analysis with Boundary Elements

journal homepage: www.elsevier.com/locate/enganabound

Generalized complex variable boundary integral equation for stress fields and torsional rigidity in torsion problems

Jia-Wei Lee [a], Hong-Ki Hong [b], Jeng-Tzong Chen [a,c,*]

[a] Department of Harbor and River Engineering, National Taiwan Ocean University, Keelung, Taiwan
[b] Department of Civil Engineering, National Taiwan University, Taipei, Taiwan
[c] Department of Mechanical and Mechatronic Engineering, National Taiwan Ocean University, Keelung, Taiwan

ARTICLE INFO

Article history:
Received 5 May 2014
Received in revised form
12 December 2014
Accepted 7 January 2015

Keywords:
Cauchy integral formula
Complex variable boundary integral equation
Holomorphic function
Complex-valued harmonic function
Stress fields
Torsional rigidity

ABSTRACT

Theory of complex variables is a very powerful mathematical technique for solving two-dimensional problems satisfying the Laplace equation. On the basis of the conventional Cauchy integral formula, the conventional complex variable boundary integral equation (CVBIE) can be constructed. The limitation is that the conventional CVBIE is only suitable for holomorphic (analytic) functions, however. To solve for a complex-valued harmonic-function pair without satisfying the Cauchy–Riemann equations, we propose a new boundary element method (BEM) based on the general Cauchy integral formula. The general Cauchy integral formula is derived by using the Borel–Pompeiu formula. The difference between the present CVBIE and the conventional CVBIE is that the former one has two boundary integrals instead of only one boundary integral in the latter one. When the unknown field is a holomorphic function, the present CVBIE can be reduced to the conventional CVBIE. Therefore, the conventional Cauchy integral formula can be viewed as a special case applicable to a holomorphic function. To examine the present CVBIE, we consider several torsion problems in this paper since the two shear stress fields satisfy the Laplace equation but do not satisfy the Cauchy–Riemann equations. Using the present CVBIE, we can directly solve the stress fields and the torsional rigidity simultaneously. Finally, several examples, including a circular bar containing an eccentric inclusion (with dissimilar materials) or hole, a circular bar, elliptical bar, equilateral triangular bar, rectangular bar, asteroid bar and circular bar with keyway, were demonstrated to check the validity of the present method.

1. Introduction

For many engineering problems, their physical phenomena can be described by certain mathematical models such as the Laplace, Helmholtz, biharmonic or biHelmholtz equation, etc. For instance, steady-state heat conduction problems [1], electrostatic potential [2], torsion problems [3], and potential flow problems [4] satisfy the Laplace equation; membrane vibration [5], water wave problems [6], acoustics [7], electromagnetic radiation [8] and seismology [9] are simulated by the Helmholtz equation; while Stokes's flow [10] and plate vibration [11] are governed by the biharmonic and biHelmholtz equations, respectively. To simulate their physical behavior, we must solve the corresponding mathematical models. For this reason, researchers and engineers paid more attention to develop various kinds of numerical methods such as the finite difference method (FDM), the finite difference method (FEM), the boundary element method (BEM), meshless methods, etc.

Although the FEM is one of the most popular methods, it costs time on constructing the geometry model and needs to generate meshes over the whole domain. In recent years, the BEM is an alternative approach to solve engineering problems. It is more efficient than the FEM since it is a mesh reduction method and only boundary discretization is required. From the viewpoint of mesh generation, the BEM [12,13] is a well-developed numerical approach for solving engineering problems with general geometries. It results in errors of geometric discretization and boundary contour integrals due to the fully populated influence matrix.

Regarding the above literatures, researchers paid more attention on the BIE and BEM in the real-variable space. The complex analysis is a very powerful mathematical technique for solving engineering problems [14]. Accordingly, Muskhelishvili [15] developed a theorem of conventional CVBIE to solve engineering problems. The conventional CVBEM [16–18] is based on the conventional Cauchy integral formula, residue theorem and Cauchy–Riemann equations in the complex analysis. For examples, applications to torsion problems [19], elasticity [20] plate problems [21], corner and crack problems [22] can be found.

* corresponding author at: Department of Harbor and River Engineering, National Taiwan Ocean University, Keelung, Taiwan. Tel.: +886 2 24622192x6177; fax: +886 2 24632375.
E-mail address: jtchen@mail.ntou.edu.tw (J.-T. Chen).

http://dx.doi.org/10.1016/j.enganabound.2015.01.003
0955-7997/

By taking the derivative for the conventional Cauchy integral formula, the Hadamard integral formula can be obtained. In this way, Chen and Chen [23] proposed the dual CVBEM to solve two-dimensional potential problems containing a degenerate boundary. It is more efficient for solving two-dimensional potential problems and plane elasticity than using the real-variables boundary element method (RVBEM) since a complex-valued function of one complex variable contains two parts. Therefore, there is a binocular view for solving an engineering problem by using the CVBEM. From the view point of mathematics, the CVBEM can deal with two field solutions for the same problem at the same time. Besides, these two field solutions are orthogonal to each other. From the view point of physics, the real part stands the potential function and the imaginary part is the stream functions for the two-dimensional potential problems.

Nevertheless, it still has a limitation. The conventional CVBEM based on the conventional Cauchy integral formula is only suitable for the holomorphic (analytic) functions. When the two unknown real-valued harmonic fields for the same problem are not the Cauchy–Riemann equation pair, the conventional one cannot be used to solve any complex-valued harmonic functions such as two shear stress fields in Saint-Venant's torsion problem. There are two ways that the two shear stress fields can be determined at once by using the conventional CVBEM. One is that Di Paola et al. [24] transformed the two shear stress fields to satisfy the Cauchy–Riemann equations by adding some terms and employed the line element-less method to solve it. Later, Barone and Pirrotta [25] used the complex polynomial method proposed by Hromadka and Guymon [26] to solve the same problem. Besides, Pirrotta [27] recently considered the shear problems in terms of a complex potential function through line integrals. Barone and Pirrotta [28] solved the problems of the same type by using the conventional CVBEM. Therefore, the conventional CVBEM can be employed to solve the two shear stress fields and the torsional rigidity at once. However, the corresponding complex-valued function is still a holomorphic function. The other way is to propose a general singular complex variable boundary integral equation (CVBIE) that is suitable for all complex-valued harmonic functions for two dimensional problems. This is the main focus of the present paper.

In this paper, we propose a general CVBEM that can be utilized to solve any complex-valued harmonic function for the two dimensional problems. We recall the Borel–Pompeiu formula [29], which is valid for essentially arbitrary complex-valued functions, and a general Cauchy integral formula for complex-valued harmonic functions [30]. On the basis of these formulae, we formulate the general singular CVBIE. Not only holomorphic functions but also complex-valued harmonic functions satisfy the general one. Thus, the corresponding general CVBEM can be developed. In this way, the general CVBEM can be employed to deal with two real-valued harmonic functions (one complex-valued harmonic function) that do not satisfy the Cauchy–Riemann equations. To check the validity of the proposed CVBEM, the two shear stress fields and the torsional rigidity of Saint-Venant's torsion problems are considered.

2. Problem statement

Let us agree with the convention: Latin indices $i,j,k=1,2,3$. For a homogeneous, isotropic, linearly elastic body $C\subseteq\mathbb{R}^3$, the governing equations may be expressed as, for $(x_1,x_2,x_3)\in C$,

$$\sigma_{ij}=G(u_{i,j}+u_{j,i})+\lambda u_{k,k}\delta_{ij}, \tag{1}$$

$$\sigma_{ij,j}+b_i=0, \tag{2}$$

where G is the shear modulus, λ is one of Lamé's constants and b_i is the x_i-component of the body force. These are a coupled system of 9 first-order partial differential equations in terms of 9 unknown functions, $u_i(x_1,x_2,x_3)$ and $\sigma_{ij}(x_1,x_2,x_3)$. For Saint-Venant's (pure) torsion problem containing an inclusion as shown in Fig. 1, a prismatic shaft is subjected to end torques M and the geometry of the shaft is $C=\Omega\times I$, ($\Omega\subseteq\mathbb{R}^2$, $I\subseteq\mathbb{R}$). The displacements are

$$u_1=-\alpha x_3x_2, \tag{3}$$

$$u_2=\alpha x_3x_1, \tag{4}$$

$$u_3=w(x_1,x_2), \tag{5}$$

and the stresses are

$$\sigma_{ij}=\begin{bmatrix}0&0&\tau_1\\0&0&\tau_2\\\tau_1&\tau_2&0\end{bmatrix}, \tag{6}$$

where α is the twist angle per unit length of the bar and $w(x_1,x_2)$ is the warping function. Equation (1) reduces to

$$\tau_1=G(w_{,1}-\alpha x_2), \tag{7}$$

$$\tau_2=G(w_{,2}+\alpha x_1). \tag{8}$$

Then, Equation (2) reduces to

$$\frac{\partial\tau_1}{\partial x_1}+\frac{\partial\tau_2}{\partial x_2}=0. \tag{9}$$

The compatibility equation for the stress fields are

$$-\frac{\partial\tau_2}{\partial x_1}+\frac{\partial\tau_1}{\partial x_2}=-2G\alpha \tag{10}$$

The process of $(\partial(9)/\partial x_2)-(\partial(10)/\partial x_1)$ gives

$$\tau_{2,jj}=0. \tag{11}$$

Similarly, the result of $(\partial(10)/\partial x_2)+(\partial(9)/\partial x_1)$ is

$$\tau_{1,jj}=0. \tag{12}$$

According to Eqs. (11) and (12), it is found that the two shear stress fields τ_2 and τ_1 are real-valued harmonic functions. In this paper, we intend to investigate the two shear stress fields directly by formulating a general Cauchy integral formula for the complex-valued harmonic function

$$f(z)=\tau_2+i\tau_1=\begin{cases}\tau_2^m+i\tau_1^m, & z\in\Omega_0,\\ \tau_2^i+i\tau_1^i, & z\in\Omega_1,\end{cases} \tag{13}$$

where

$$z=x_1+ix_2, \tag{14}$$

the superscripts "m" and "i" denote the matrix and inclusion, respectively, and Ω_0 and Ω_1 stand for the domain of the cross section for the matrix and inclusion, respectively. However, it should be noted that the above complex-valued function does not satisfy the Cauchy–Riemann equations since the right hand side of the compatibility equation in Eq. (10) is not equal to zero. Note that $f(z)$ is a complex-valued harmonic function, rather than a holomorphic function. That is to say, τ_2 and τ_1 satisfy only one of

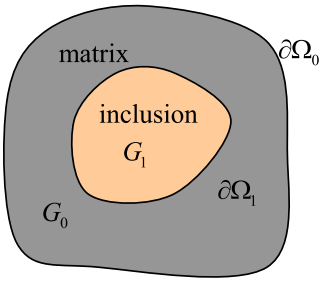

Fig. 1. The cross-section of a torsion bar containing an inclusion.

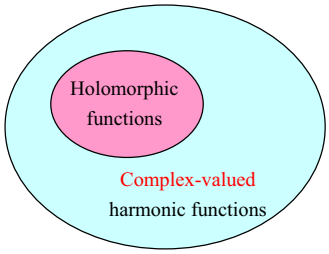

Fig. 2. The sketch of relation between the set of holomorphic functions and complex-valued harmonic functions.

the Cauchy–Riemann pair. The set of complex-valued harmonic functions includes the set of holomorphic functions and their relationship is shown in Fig. 2. For this reason, the conventional CVBIE based on the conventional Cauchy integral formula is not suitable for solving a complex-valued harmonic function. In this paper, we propose a general Cauchy integral formula that can be employed to solve all complex-valued harmonic functions. Since no external forces act on the lateral surface of the bar, we have the traction free boundary condition as given below

$$(\tau_1^m, \tau_2^m)\cdot(n_1^m, n_2^m) = \tau_1^m n_1^m + \tau_2^m n_2^m = 0, \quad z \in \partial\Omega_0, \tag{15}$$

where n_1^m and n_2^m are the horizontal and vertical components of the unit outward normal vector along the outer boundary $\partial\Omega_0$, respectively. The static equivalence condition for the torque M is defined as

$$M = \iint_\Omega (-x_2\tau_1 + x_1\tau_2)dx_1\, dx_2, \quad z \in \overline{\Omega}, \tag{16}$$

where Ω stands for the all domain of the cross section. Besides, we can obtain the second boundary condition in terms of the complex function $f(z)$ from Eqs. (10) and (11) as shown below

$$\frac{\partial f(z)}{\partial \bar{z}} = G\alpha, \quad z \in \overline{\Omega}. \tag{17}$$

The interface condition for the ideal boundary between the matrix and the inclusion, we have the continuity condition of the warping function

$$w^m = w^i, \quad z \in \partial\Omega_1, \tag{18}$$

and the equilibrium condition for the normal traction

$$(\tau_1^m, \tau_2^m)\cdot(n_1^m, n_2^m) + (\tau_1^i, \tau_2^i)\cdot(n_1^i, n_2^i) = 0, \quad z \in \partial\Omega_1, \tag{19}$$

where $(n_1^m, n_2^m) = -(n_1^i, n_2^i)$.

3. Derivation of the general Cauchy integral formula

In this section, we derive the general Cauchy integral formula in terms of boundary integrals starting from the Borel–Pompeiu formula [29]. First, we revisit the Borel–Pompeiu formula. The Gauss theorem for the two-dimensional case is

$$\int_\Omega \nabla\cdot(u,v)dA = \int_{\partial\Omega}(u,v)\cdot\mathbf{n}\, dS, \tag{20}$$

where ∇ is the gradient operator, $\mathbf{n}$ is the unit outward normal vector field along the boundary, and u and v are real-valued functions. In complex analysis, from the above equation we can obtain the complex-valued form of the Gauss theorem,

$$\int_\Omega \frac{\partial w(s)}{\partial \bar{s}} ds_1\, ds_2 = \frac{1}{2i}\int_{\partial\Omega} w(s)ds, \tag{21}$$

and its conjugate form

$$\int_\Omega \frac{\partial w(s)}{\partial s} ds_1\, ds_2 = -\frac{1}{2i}\int_{\partial\Omega} w(s)d\bar{s}, \tag{22}$$

where $s = s_1 + is_2$ and $w(s) = u(s) + iv(s)$ is a complex-valued function. Substituting $w(s) = (f(s)/s - z)$ into Eq. (21), we have the Borel–Pompeiu formula for $z \in \mathbb{C}\backslash\overline{\Omega}$,

$$0 = \frac{1}{2i}\int_{\partial\Omega}\frac{f(s)}{s-z}ds - \int_\Omega \frac{1}{s-z}\frac{\partial f(s)}{\partial \bar{s}} ds_1\, ds_2. \tag{23}$$

Then substituting $(\partial f(s)/\partial\bar{s})\ln|s-z|^2$ for $w(s)$ in Eq. (22), we have

$$-\int_\Omega \frac{1}{s-z}\frac{\partial f(s)}{\partial \bar{s}} ds_1\, ds_2 = \frac{1}{2i}\int_{\partial\Omega}\frac{\partial f(s)}{\partial \bar{s}}\ln|s-z|^2 d\bar{s} + \int_\Omega \frac{\partial^2 f(s)}{\partial\bar{s}\partial s}\ln|s-z|^2 ds_1\, ds_2, \tag{24}$$

where $f(s) \in C^1(\overline{\Omega}) \cap C^2(\Omega)$. Substituting Eq. (24) into Eq. (23), we have

$$0 = \frac{1}{2i}\int_{\partial\Omega}\frac{f(s)}{s-z}ds + \frac{1}{2i}\int_{\partial\Omega}\frac{\partial f(s)}{\partial \bar{s}}\ln|s-z|^2\, d\bar{s} + \int_\Omega \frac{\partial^2 f(s)}{\partial\bar{s}\partial s}\ln|s-z|^2 ds_1\, ds_2. \tag{25}$$

If $f(s)$ satisfies the two-dimensional Laplace equation $(\partial^2 f(s)/\partial\bar{s}\partial s) = 0$, *i.e.*, $f(s)$ is a complex-valued harmonic function, the area integral in Eq. (25) vanishes. Therefore, we have

$$0 = \frac{1}{2i}\int_{\partial\Omega}\frac{f(s)}{s-z}ds + \frac{1}{2i}\int_{\partial\Omega}\frac{\partial f(s)}{\partial \bar{s}}\ln|s-z|^2\, d\bar{s}. \tag{26}$$

When $z \in \Omega$, a singular point exists in the domain Ω in Eq. (26). To deal with this problem to obtain the general Cauchy integral formula in terms of boundary integrals for $z \in \Omega$, we need to employ the limiting process. In this way, we obtain

$$f(z) = \frac{1}{2\pi i}\int_{\partial\Omega}\frac{f(s)}{s-z}ds + \frac{1}{2\pi i}\int_{\partial\Omega}\frac{\partial f(s)}{\partial \bar{s}}\ln|s-z|^2\, d\bar{s}, \quad z \in \Omega. \tag{27}$$

If the field point z is outside the domain ($z \in \mathbb{C}\backslash\overline{\Omega}$), we can also obtain the general Cauchy integral formula for the null field point from Eq. (27) as follows:

$$0 = \frac{1}{2\pi i}\int_{\partial\Omega}\frac{f(s)}{s-z}ds + \frac{1}{2\pi i}\int_{\partial\Omega}\frac{\partial f(s)}{\partial \bar{s}}\ln|s-z|^2\, d\bar{s}, \quad z \in \mathbb{C}\backslash\overline{\Omega}. \tag{28}$$

If the field point z is located on the boundary ($z \in \partial\Omega$), Eq. (28) yields the singularity since $z = s$ may occur. Therefore, we also need to employ the limiting process and introduce the concept of Cauchy principal value. Then, we have,

$$\frac{\alpha}{2\pi}f(z) = \frac{1}{2\pi i}C.P.V.\int_{\partial\Omega}\frac{f(s)}{s-z}ds + \frac{1}{2\pi i}\int_{\partial\Omega}\frac{\partial f(s)}{\partial \bar{s}}\ln|s-z|^2\, d\bar{s}, \quad z \in \partial\Omega, \tag{29}$$

where α is the solid angle and the *C.P.V.* stands for the Cauchy principal value. Summarizing Eqs. (27)–(29), we have

$$c(z)f(z) = \frac{1}{2\pi i}\int_{\partial\Omega}^{(z)}\frac{f(s)}{s-z}ds + \frac{1}{2\pi i}\int_{\partial\Omega}\frac{\partial f(s)}{\partial \bar{s}}\ln|s-z|^2\, d\bar{s}, \tag{30}$$

where

$$c(z) = \begin{cases} 1, & z \in \Omega, \\ \frac{\alpha}{2\pi}, & z \in \partial\Omega, \\ 0, & z \in \mathbb{C}\backslash\overline{\Omega}, \end{cases} \tag{31}$$

and

$$\int_{\partial\Omega}^{(z)} = \begin{cases} \int_{\partial\Omega}, & z \in \Omega, \\ C.P.V.\int_{\partial\Omega}, & z \in \partial\Omega, \\ \int_{\partial\Omega}, & z \in \mathbb{C}\backslash\overline{\Omega}. \end{cases} \tag{32}$$

Eq. (30) is the so-called general Cauchy integral formula in terms of boundary integral. Note that all of complex-valued harmonic functions satisfy Eq. (30). If the complex-valued function $f(z)$ is a holomorphic function ($(\partial f(z)/\partial\bar{z}) = 0$), the general Cauchy integral formula can be reduced to the conventional Cauchy integral formula. Therefore, the conventional Cauchy integral

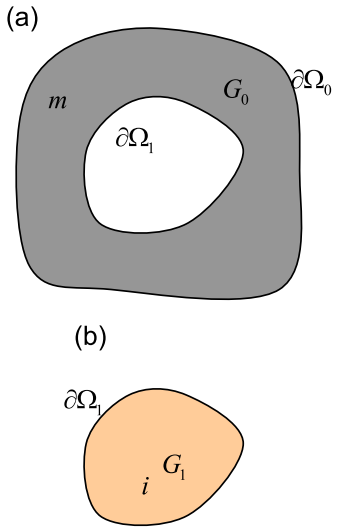

Fig. 3. Each cross-section of a torsion bar containing an inclusion. (a) Matrix and (b) Inclusion

formula can be viewed as a special case applicable to a holomorphic function. Besides, when we employ the general Cauchy integral formula to solve a complex-valued harmonic function, this formula can be known as the general complex variable boundary integral equation (CVBIE).

4. Application of general Cauchy integral formula for a torsion bar containing an inclusion

According to the concept of domain decomposition, the torsion problem containing an inclusion in Fig. 1 can be decomposed into two subdomains as shown in Fig. 3(a) and (b). One is the part of the matrix and the other is the part of the inclusion. For the first part as shown in Fig. 3(a), we have two following CVBIEs for the collocation point on the boundary $\partial\Omega_0$ or $\partial\Omega_1$,

$$\frac{\alpha}{2\pi}f_0^m(z)=\frac{C.P.V.}{2\pi i}\int_{\partial\Omega_0}\frac{\partial \ln|s-z|^2}{\partial s}f_0^m(s)ds+\frac{1}{2\pi i}\int_{\partial\Omega_1}\frac{\partial \ln|s-z|^2}{\partial s}f_1^m(s)ds$$
$$+\frac{1}{2\pi i}\int_{\partial\Omega_0}\ln|s-z|^2\frac{\partial f_0^m(s)}{\partial \bar{s}}d\bar{s}+\frac{1}{2\pi i}\int_{\partial\Omega_1}\ln|s-z|^2\frac{\partial f_1^m(s)}{\partial \bar{s}}d\bar{s},$$
$$z\in\partial\Omega_0, \tag{33}$$

$$\frac{\alpha}{2\pi}f_1^m(z)=\frac{1}{2\pi i}\int_{\partial\Omega_0}\frac{\partial \ln|s-z|^2}{\partial s}f_0^m(s)ds+\frac{C.P.V.}{2\pi i}\int_{\partial\Omega_1}\frac{\partial \ln|s-z|^2}{\partial s}f_1^m(s)ds$$
$$+\frac{1}{2\pi i}\int_{\partial\Omega_0}\ln|s-z|^2\frac{\partial f_0^m(s)}{\partial \bar{s}}d\bar{s}+\frac{1}{2\pi i}\int_{\partial\Omega_1}\ln|s-z|^2\frac{\partial f_1^m(s)}{\partial \bar{s}}d\bar{s},\quad z\in\partial\Omega_1, \tag{34}$$

where $f_0^m(\cdot)$ and $f_1^m(\cdot)$ stand for the two shear stresses along $\partial\Omega_0$ and $\partial\Omega_1$ of the matrix, respectively. Similarly for the second part as shown in Fig. 3(b), we also have the CVBIE for the collocation point on the boundary $\partial\Omega_1$,

$$\frac{\alpha}{2\pi}f_1^i(z)=\frac{C.P.V.}{2\pi i}\int_{\partial\Omega_1}\frac{\partial \ln|s-z|^2}{\partial s}f_1^i(s)ds+\frac{1}{2\pi i}\int_{\partial\Omega_1}\ln|s-z|^2\frac{\partial f_1^i(s)}{\partial \bar{s}}d\bar{s},\quad z\in\partial\Omega_1, \tag{35}$$

where $f_1^i(\cdot)$ stands for the two shear stresses along $\partial\Omega_1$ of the inclusion.

5. Discretization of the complex variable boundary integral equations and matching of boundary conditions

In this section, we employ the constant element scheme to discretize the CVBIEs of Eqs. (33)–(35) in the following:

$$\tfrac{1}{2}\{\mathbf{f}_0^m\}=\left[\tilde{\mathbf{T}}_{00}^m\right]\{\mathbf{f}_0^m\}+[\mathbf{T}_{01}^m]\{\mathbf{f}_1^m\}+[\mathbf{U}_{00}^m]\{\mathbf{g}_0^m\}+[\mathbf{U}_{01}^m]\{\mathbf{g}_1^m\}, \tag{36}$$

$$\tfrac{1}{2}\{\mathbf{f}_1^m\}=[\mathbf{T}_{10}^m]\{\mathbf{f}_0^m\}+\left[\tilde{\mathbf{T}}_{11}^m\right]\{\mathbf{f}_1^m\}+[\mathbf{U}_{10}^m]\{\mathbf{g}_0^m\}+[\mathbf{U}_{11}^m]\{\mathbf{g}_1^m\}, \tag{37}$$

$$\tfrac{1}{2}\left\{\mathbf{f}_1^i\right\}=\left[\tilde{\mathbf{T}}_{11}^i\right]\left\{\mathbf{f}_1^i\right\}+\left[\mathbf{U}_{11}^i\right]\left\{\mathbf{g}_1^i\right\}. \tag{38}$$

Note that the Cauchy principal value needs to be considered for the diagonal elements in the influence matrices $\left[\tilde{\mathbf{T}}_{00}^m\right]$, $\left[\tilde{\mathbf{T}}_{11}^m\right]$ and $\left[\tilde{\mathbf{T}}_{11}^i\right]$. After arrangement for Eqs. (36)–(38), we have

$$[\mathbf{T}_{00}^m]\{\mathbf{f}_0^m\}+[\mathbf{T}_{01}^m]\{\mathbf{f}_1^m\}+[\mathbf{U}_{00}^m]\{\mathbf{g}_0^m\}+[\mathbf{U}_{01}^m]\{\mathbf{g}_1^m\}=\{0\}_{N_0\times 1}, \tag{39}$$

$$[\mathbf{T}_{10}^m]\{\mathbf{f}_0^m\}+[\mathbf{T}_{11}^m]\{\mathbf{f}_1^m\}+[\mathbf{U}_{10}^m]\{\mathbf{g}_0^m\}+[\mathbf{U}_{11}^m]\{\mathbf{g}_1^m\}=\{0\}_{N_1\times 1}, \tag{40}$$

$$\left[\mathbf{T}_{11}^i\right]\left\{\mathbf{f}_1^i\right\}+\left[\mathbf{U}_{11}^i\right]\left\{\mathbf{g}_1^i\right\}=\{0\}_{N_1\times 1}, \tag{41}$$

where

$$\{\mathbf{f}_0^m\}=\{f_{0l}^m\}_{N_0\times 1},\quad \{\mathbf{f}_1^m\}=\{f_{1l}^m\}_{N_1\times 1},\quad \left\{\mathbf{f}_1^i\right\}=\left\{f_{1l}^i\right\}_{N_1\times 1} \tag{42}$$

$$\{\mathbf{g}_0^m\}=\{g_{0l}^m\}_{N_0\times 1},\quad \{\mathbf{g}_1^m\}=\{g_{1l}^m\}_{N_1\times 1},\quad \left\{\mathbf{g}_1^i\right\}=\left\{g_{1l}^i\right\}_{N_1\times 1} \tag{43}$$

$$[\mathbf{T}_{rv}]=\left[T_{rv}^{jl}\right],\quad [\mathbf{U}_{rv}]=\left[U_{rv}^{jl}\right], \tag{44}$$

where N_0 and N_1 are the number of elements on boundaries $\partial\Omega_0$ and $\partial\Omega_1$, respectively. The subscript r in $[\mathbf{T}_{rv}]$ stands for the index the rth boundary where the collocation point is located and the subscript v in $[\mathbf{U}_{rv}]$ stands for the index of the vth boundary where the path of boundary integral is considered. Each element in influence matrices $\left[T_{rv}^{jl}\right]$ and $\left[U_{rv}^{jl}\right]$ is determined by

$$T_{rv}^{jl}=\begin{cases}\frac{1}{2\pi i}C.P.V.\int_{\partial\Omega_l}\frac{1}{s_l-z_j}ds_l-\frac{1}{2}=0, & (r=v)\cap(j=l),\\ \frac{1}{2\pi i}\int_{\partial\Omega_l}\frac{1}{s_l-z_j}ds_l=\frac{1}{2\pi i}\ln(s_l-z_j)\big|_{s_l=s_l^L}^{s_l=s_l^R}, & (r\neq v)\cup(j\neq l),\end{cases} \tag{45}$$

$$U_{rv}^{jl}=\frac{1}{2\pi i}\int_{\partial\Omega_l}\ln|s_l-z_j|^2\,ds_l=\frac{e^{-i\theta_l}}{\pi i}\int_{\partial\Omega_l}\ln|s_l-z_j|dt(s_l), \tag{46}$$

where s_l^L and s_l^R are the coordinates of the starting and ending points for the lth element, respectively, θ_l and $dt(s_l)$ are the azimuth and the path integral of the lth element, respectively, and

$$g_{0l}^m=\left.\frac{\partial f_0^m(s)}{\partial \bar{s}}\right|_{s=s_l}=G_0\alpha, \tag{47}$$

$$g_{1l}^m=\left.\frac{\partial f_1^m(s)}{\partial \bar{s}}\right|_{s=s_l}=G_0\alpha, \tag{48}$$

$$g_{1l}^i=\left.\frac{\partial f_1^i(s)}{\partial \bar{s}}\right|_{s=s_l}=G_1\alpha. \tag{49}$$

After substituting the boundary condition in Eqs. (47)–(49) to Eqs. (39)–(41), we have

$$[\mathbf{T}_{00}^m]\{\mathbf{f}_0^m\}+[\mathbf{T}_{01}^m]\{\mathbf{f}_1^m\}+G_0\alpha\{\mathbf{p}_0^m\}=\{0\}_{N_0\times 1}, \tag{50}$$

$$[\mathbf{T}_{10}^m]\{\mathbf{f}_0^m\}+[\mathbf{T}_{11}^m]\{\mathbf{f}_1^m\}+G_0\alpha\{\mathbf{p}_1^m\}=\{0\}_{N_1\times 1}, \tag{51}$$

$$\left[\mathbf{T}_{11}^i\right]\left\{\mathbf{f}_1^i\right\}+G_1\alpha\left\{\mathbf{p}_1^i\right\}=\{0\}_{N_1\times 1}, \tag{52}$$

where

$$\{\mathbf{p}_0^m\} = [\mathbf{U}_{00}^m]\{1\} + [\mathbf{U}_{01}^m]\{1\}, \tag{53}$$

$$\{\mathbf{p}_1^m\} = [\mathbf{U}_{10}^m]\{1\} + [\mathbf{U}_{11}^m]\{1\}, \tag{54}$$

$$\left\{\mathbf{p}_1^i\right\} = \left[\mathbf{U}_{11}^i\right]\{1\}. \tag{55}$$

To satisfy the traction free condition on the boundary $\partial\Omega_0$, we can assume

$$f_0^m(z) = \overline{n}_0^m(z)\beta_0^m(z), \quad \overline{n}_0^m(z) = n_{01}^m - in_{02}^m, \quad z \in \partial\Omega_0, \tag{56}$$

where (n_{01}^m, n_{02}^m) is the unit outward normal vector along the boundary $\partial\Omega_0$ and

$$\beta_0^m(z) = (\tau_{01}^m, \tau_{02}^m)\cdot(n_{01}^m, n_{02}^m), \quad z \in \partial\Omega_0, \tag{57}$$

is the tangential traction along the boundary $\partial\Omega_0$. In this way, the traction free boundary condition on the boundary $\partial\Omega_0$ is automatically satisfied. Also using the constant element scheme to discretize Eq. (56), we have

$$\{\mathbf{f}_0^m\} = [\overline{\mathbf{n}}_0^m]\{\boldsymbol{\beta}_0^m\}, \tag{58}$$

where

$$\{\boldsymbol{\beta}_0^m\} = \{\beta_{0l}^m\}, \quad l = 1, 2, \ldots, N_0, \tag{59}$$

$$[\overline{\mathbf{n}}_0^m] = \left[\overline{n}_{0jl}^m\right]_{N_0\times N_0}, \tag{60}$$

where $\left[\overline{n}_{0jl}^m\right]$ is a diagonal matrix as given below

$$\overline{n}_{0jl}^m = \begin{cases} \overline{n}_0^m(z_j), & j = l, \\ 0, & j \neq l. \end{cases} \tag{61}$$

Similarly, we have

$$f_1^m(z) = \overline{n}_1^m(z)\beta_1^m(z) + i\overline{n}_1^m(z)\tau_n^m(z), \quad z \in \partial\Omega_1, \tag{62}$$

$$f_1^i(z) = \overline{n}_1^i(z)\beta_1^i(z) + i\overline{n}_1^i(z)\tau_n^i(z), \quad z \in \partial\Omega_1, \tag{63}$$

where

$$\overline{n}_1^m(z) = -\overline{n}_1^i(z), \quad z \in \partial\Omega_1, \tag{64}$$

$\tau_n^m(z)$ and $\tau_n^i(z)$ are the normal tractions along the boundary $\partial\Omega_1$ in the domains of $\partial\Omega_0$ and $\partial\Omega_1$. After using the constant element scheme to discretize Eqs. (62) and (63), we have

$$\{\mathbf{f}_1^m\} = [\overline{\mathbf{n}}_1^m]\{\boldsymbol{\beta}_1^m\} + i[\overline{\mathbf{n}}_1^m]\{\boldsymbol{\tau}_n^m\}, \tag{65}$$

$$\left\{\mathbf{f}_1^i\right\} = \left[\overline{\mathbf{n}}_1^i\right]\left\{\boldsymbol{\beta}_1^i\right\} + i\left[\overline{\mathbf{n}}_1^i\right]\left\{\boldsymbol{\tau}_n^i\right\}, \tag{66}$$

where

$$\{\boldsymbol{\beta}_1^m\} = \{\beta_{1l}^m\}, \quad \{\boldsymbol{\tau}_n^m\} = \{\tau_{nl}^m\}, \quad \left\{\boldsymbol{\beta}_1^i\right\} = \left\{\beta_{1l}^i\right\}, \quad \left\{\boldsymbol{\tau}_n^i\right\} = \left\{\tau_{nl}^i\right\}, \quad l = 1, 2, \ldots, N_1, \tag{67}$$

$$[\overline{\mathbf{n}}_1^m] = -\left[\overline{\mathbf{n}}_1^i\right] = \left[\overline{n}_{1jl}^m\right]_{N_1\times N_1}, \tag{68}$$

where $\left[\overline{n}_{1jl}^m\right]$ is a diagonal matrix as given below

$$\overline{n}_{1jl}^m = \begin{cases} \overline{n}_1^m(z_j), & j = l, \\ 0, & j \neq l. \end{cases} \tag{69}$$

Substituting Eqs. (58) and (65) to Eqs. (50) and (51), we have

$$[\mathbf{T}_{00}^m\overline{\mathbf{n}}_0^m]\{\boldsymbol{\beta}_0^m\} + [\mathbf{T}_{01}^m\overline{\mathbf{n}}_1^m]\{\boldsymbol{\beta}_1^m\} + i[\mathbf{T}_{01}^m\overline{\mathbf{n}}_1^m]\{\boldsymbol{\tau}_n^m\} + G_0\alpha\{\mathbf{p}_0^m\} = \{0\}_{N_0\times 1}, \tag{70}$$

$$[\mathbf{T}_{10}^m\overline{\mathbf{n}}_0^m]\{\boldsymbol{\beta}_0^m\} + [\mathbf{T}_{11}^m\overline{\mathbf{n}}_1^m]\{\boldsymbol{\beta}_1^m\} + i[\mathbf{T}_{11}^m\overline{\mathbf{n}}_1^m]\{\boldsymbol{\tau}_n^m\} + G_0\alpha\{\mathbf{p}_1^m\} = \{0\}_{N_1\times 1}. \tag{71}$$

Similarly, substituting Eq. (66) in Eq. (52), we have

$$\left[\mathbf{T}_{11}^i\overline{\mathbf{n}}_1^i\right]\left\{\boldsymbol{\beta}_1^i\right\} + i\left[\mathbf{T}_{11}^i\overline{\mathbf{n}}_1^i\right]\left\{\boldsymbol{\tau}_n^i\right\} + G_1\alpha\left\{\mathbf{p}_1^i\right\} = \{0\}_{N_1\times 1}. \tag{72}$$

According to the continuity condition of the warping function and the equilibrium condition for the normal traction, we have

$$\frac{G_1}{G_0}\beta_1^m(z) + \beta_1^i(z) = 0, \quad z \in \partial\Omega_1, \tag{73}$$

$$\tau_n^m(z) + \tau_n^i(z) = 0, \quad z \in \partial\Omega_1. \tag{74}$$

After discretizing Eqs. (73) and (74) by employing the constant element scheme, we have

$$\frac{G_1}{G_0}[\mathrm{I}]\{\boldsymbol{\beta}_1^m\} + [\mathbf{I}]^A\left\{\boldsymbol{\beta}_1^i\right\} = \{0\}_{N_1\times 1}, \tag{75}$$

$$[\mathbf{I}]\{\boldsymbol{\tau}_n^m\} + [\mathbf{I}]^A\left\{\boldsymbol{\tau}_n^i\right\} = \{0\}_{N_1\times 1}. \tag{76}$$

Since the distributions of the elements along the boundary $\partial\Omega_1$ in the matrix and the inclusion are counterclockwise and clockwise, respectively, $[\mathbf{I}]$ and $[\mathbf{I}]^A$ stand for the identity matrix and the anti-identity matrix.

Furthermore, to easily calculate the static equivalence condition, we transform it into the form of contour integrals as shown below

$$M = \int_{\partial\Omega_0} F\beta_0^m(z)dt(z) + \int_{\partial\Omega_1} F\beta_1^m(z)dt(z) + \int_{\partial\Omega_1} F\beta_1^i(z)dt(z) - G_0\alpha I_{p_0} - G_1\alpha I_{p_1}, \tag{77}$$

where

$$F = \tfrac{1}{2}z\bar{z}, \tag{78}$$

I_{p_0} and I_{p_1} are the polar moments of inertia of the areas Ω_0 and Ω_1, respectively. Also, we employ the constant element scheme to discretize the static equivalence condition in Eq. (77) and we have

$$\{\mathbf{q}_0^m\}^T\{\boldsymbol{\beta}_0^m\} + \{\mathbf{q}_1^m\}^T\{\boldsymbol{\beta}_1^m\} + \left\{\mathbf{q}_1^i\right\}^T\left\{\boldsymbol{\beta}_1^i\right\} - G_0\alpha I_{p_0} - G_1\alpha I_{p_1} = M, \tag{79}$$

where

$$\{\mathbf{q}_0^m\} = \left\{q_{0j}^m\right\}_{1\times N_0}, \quad \{\mathbf{q}_1^m\} = \left\{q_{1j}^m\right\}_{1\times N_1}, \quad \left\{\mathbf{q}_1^i\right\} = \left\{q_{1j}^i\right\}_{1\times N_1}, \tag{80}$$

in which

$$q_j = \frac{1}{2}\int_{\partial\Omega_j} z\bar{z}\, dt(z_j). \tag{81}$$

Furthermore, to ensure the warping function to be single-valued, we have the three external constraint equations

$$\int_{\partial\Omega_0} \beta_0^m(z)dt(z) - 2G_0\alpha A_0 = 0, \tag{82}$$

$$\int_{\partial\Omega_1} \beta_1^m(z)dt(z) - 2G_0\alpha A_1 = 0, \tag{83}$$

$$\int_{\partial\Omega_1} \beta_1^i(z)dt(z) - 2G_1\alpha A_1 = 0, \tag{84}$$

where A_0 and A_1 stand for the areas of the matrix and inclusion, respectively. After discretization Eqs. (82)–(84), we have

$$\{\mathbf{l}_0^m\}^T\{\boldsymbol{\beta}_0^m\} - 2G_0\alpha A_0 = 0, \tag{85}$$

$$\{\mathbf{l}_1^m\}^T\{\boldsymbol{\beta}_1^m\} - 2G_0\alpha A_1 = 0, \tag{86}$$

$$\left\{\mathbf{l}_1^i\right\}^T\left\{\boldsymbol{\beta}_1^i\right\} - 2G_1\alpha A_1 = 0, \tag{87}$$

where

$$\{\mathbf{l}_0^m\} = \{l_{1l}^m\}, \quad \{\mathbf{l}_1^m\} = \{l_{1l}^m\}, \quad \left\{\mathbf{l}_1^i\right\} = \left\{l_{1l}^i\right\}, \tag{88}$$

where l is the length of the element.

Then we have the following linear algebraic equation by combining Eqs. (70)–(72), (75), (76), (79), (85)–(87):

$$[\mathbf{A}]\{\mathbf{x}\}=\{\mathbf{b}\}, \tag{89}$$

where

$$[\mathbf{A}]=\begin{bmatrix} [\mathbf{T}_{00}^m\bar{\mathbf{n}}_0^m] & [\mathbf{T}_{01}^m\bar{\mathbf{n}}_1^m] & i[\mathbf{T}_{01}^m\bar{\mathbf{n}}_1^m] & 0 & 0 & G_0\{\mathbf{p}_0^m\} \\ [\mathbf{T}_{10}^m\bar{\mathbf{n}}_0^m] & [\mathbf{T}_{11}^m\bar{\mathbf{n}}_1^m] & i[\mathbf{T}_{11}^m\bar{\mathbf{n}}_1^m] & 0 & 0 & G_0\{\mathbf{p}_1^m\} \\ 0 & 0 & 0 & \left[\mathbf{T}_{11}^i\bar{\mathbf{n}}_1^i\right] & i\left[\mathbf{T}_{11}^i\bar{\mathbf{n}}_1^i\right] & G_1\{\mathbf{p}_1^i\} \\ 0 & \frac{G_1}{G_0}[\mathbf{I}] & 0 & [\mathbf{I}]^A & 0 & 0 \\ 0 & 0 & [\mathbf{I}] & 0 & [\mathbf{I}]^A & 0 \\ \{\mathbf{q}_0^m\}^T & \{\mathbf{q}_1^m\}^T & 0 & \{\mathbf{q}_1^i\}^T & 0 & -G_0I_{p_0}-G_1I_{p_1} \\ \{\mathbf{l}_0^m\}^T & 0 & 0 & 0 & 0 & -2G_0A_0 \\ 0 & \{\mathbf{l}_1^m\}^T & 0 & 0 & 0 & -2G_0A_1 \\ 0 & 0 & 0 & \left\{\mathbf{l}_1^i\right\}^T & 0 & -2G_1A_1 \end{bmatrix}, \tag{90}$$

$$\{\mathbf{x}\}=\begin{Bmatrix} \boldsymbol{\beta}_0^m \\ \boldsymbol{\beta}_1^m \\ \boldsymbol{\tau}_n^m \\ \boldsymbol{\beta}_1^i \\ \boldsymbol{\tau}_n^i \\ \alpha \end{Bmatrix}, \tag{91}$$

and

$$\{\mathbf{b}\}=\begin{Bmatrix} 0\\0\\0\\0\\0\\M\\0\\0\\0 \end{Bmatrix}. \tag{92}$$

To ensure the influence matrix in Eq. (89) to be of full rank, we update it to be

$$\left[\tilde{\mathbf{A}}\right]\{\mathbf{x}\}=\left\{\tilde{\mathbf{b}}\right\}, \tag{93}$$

where

$$\left\{\tilde{\mathbf{b}}\right\}=\begin{Bmatrix} 0\\0\\0\\0\\0\\0\\0\\M\\0\\0\\0 \end{Bmatrix}. \tag{95}$$

Note that all elements of the influence matrix in Eq. (94) are real-valued. Since the influence matrice is over-determined, we employed the pseudoinverse matrix method to evaluate its inverse matrix. Regarding the present approach for solving the torsion problems, the torsional rigidity, D, can be straightforward obtained as expressed below

$$D=\frac{M}{\alpha}. \tag{96}$$

Without loss of generality, we set the torque M to be 1 in the real implementation.

6. Numerical examples and discussions

In this paper, we consider three situations of the torsion problem to demonstrate the validity of the present approach. The first one is the case of inclusion, the second one is a hollow case and the final one is a solid case.

6.1. A circular bar containing an eccentric inclusion

First, a circular torsion bar containing an eccentric inclusion is considered as shown in Fig. 4(a). The radii of the outer circular and inner circular are $a_0=1$ and $a_1=0.3$, respectively. The eccentric distance is $e_1=0.6$. The dimensionless ratios of the torsional rigidity versus different ratio of G_1/G_0 are shown in Table 1. Besides, the exact solutions derived by Muskhelishvili [14], semi-analytical solutions obtained from Chen and Lee [31], and the

$$\left[\tilde{\mathbf{A}}\right]=\begin{bmatrix} \mathrm{Re}[\mathbf{T}_{00}^m\bar{\mathbf{n}}_0^m] & \mathrm{Re}[\mathbf{T}_{01}^m\bar{\mathbf{n}}_1^m] & \mathrm{Re}[i\mathbf{T}_{01}^m\bar{\mathbf{n}}_1^m] & 0 & 0 & \mathrm{Re}(G_0\{\mathbf{p}_0^m\}) \\ \mathrm{Im}[\mathbf{T}_{00}^m\bar{\mathbf{n}}_0^m] & \mathrm{Im}[\mathbf{T}_{01}^m\bar{\mathbf{n}}_1^m] & \mathrm{Im}[i\mathbf{T}_{01}^m\bar{\mathbf{n}}_1^m] & 0 & 0 & \mathrm{Im}(G_0\{\mathbf{p}_0^m\}) \\ \mathrm{Re}[\mathbf{T}_{10}^m\bar{\mathbf{n}}_0^m] & \mathrm{Re}[\mathbf{T}_{11}^m\bar{\mathbf{n}}_1^m] & \mathrm{Re}[i\mathbf{T}_{11}^m\bar{\mathbf{n}}_1^m] & 0 & 0 & \mathrm{Re}(G_0\{\mathbf{p}_1^m\}) \\ \mathrm{Im}[\mathbf{T}_{10}^m\bar{\mathbf{n}}_0^m] & \mathrm{Im}[\mathbf{T}_{11}^m\bar{\mathbf{n}}_1^m] & \mathrm{Im}[i\mathbf{T}_{11}^m\bar{\mathbf{n}}_1^m] & 0 & 0 & \mathrm{Im}(G_0\{\mathbf{p}_1^m\}) \\ 0 & 0 & 0 & \mathrm{Re}\left[\mathbf{T}_{11}^i\bar{\mathbf{n}}_1^i\right] & \mathrm{Re}\left[i\mathbf{T}_{11}^i\bar{\mathbf{n}}_1^i\right] & \mathrm{Re}(G_1\{\mathbf{p}_1^i\}) \\ 0 & 0 & 0 & \mathrm{Im}\left[\mathbf{T}_{11}^i\bar{\mathbf{n}}_1^i\right] & \mathrm{Im}\left[i\mathbf{T}_{11}^i\bar{\mathbf{n}}_1^i\right] & \mathrm{Im}(G_1\{\mathbf{p}_1^i\}) \\ 0 & \frac{G_1}{G_0}[\mathbf{I}] & 0 & [\mathbf{I}]^A & 0 & 0 \\ 0 & 0 & [\mathbf{I}] & 0 & [\mathbf{I}]^A & 0 \\ \{\mathbf{q}_0^m\}^T & \{\mathbf{q}_1^m\}^T & 0 & \{\mathbf{q}_1^i\}^T & 0 & -G_0I_{p_0}-G_1I_{p_1} \\ \{\mathbf{l}_0^m\}^T & 0 & 0 & 0 & 0 & -2G_0A_0 \\ 0 & \{\mathbf{l}_1^m\}^T & 0 & 0 & 0 & -2G_0A_1 \\ 0 & 0 & 0 & \left\{\mathbf{l}_1^i\right\}^T & 0 & -2G_1A_1 \end{bmatrix}, \tag{94}$$

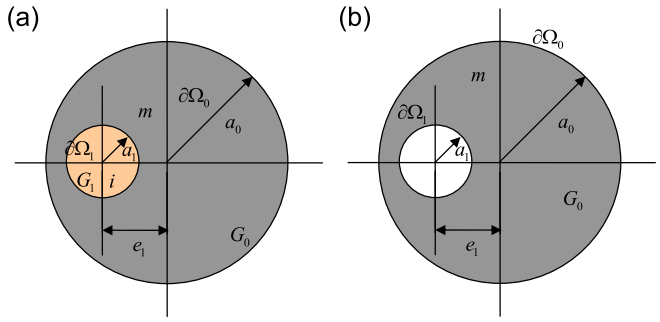

Fig. 4. The cross-section of a circular bar containing an eccentric inclusion or a hole. (a) The case of an inclusion and (b) Eccentric case

Table 1
Torsional rigidity for a circular bar containing an eccentric inclusion.

$\frac{G_1}{G_0}$	$2D/\pi G_0 a_0^4$			
	Present	Chen and Lee [31]	Muskhelishvili [14]	Tang [32]
0	0.83520 (1.40%)	0.82370	0.82370	0.82377
0.2	0.89898 (0.81%)	0.89180	0.89180	0.89181
0.6	0.96874 (0.62%)	0.96246	0.96246	0.96246
1.0	1.00659 (0.66%)	1.00000	1.00000	1.00000
5.0	1.11797 (0.90%)	1.10800	1.10800	1.10794
20.0	1.27250 (1.62%)	1.25224	1.25224	1.25181

Table 2
Torsional rigidity for a circular bar containing an eccentric hole.

$\frac{e_0}{a_0-a_1}$	$2D/\pi G_0 a_0^4$		
	Present	Chen et al. [33]	Muskhelishvili [14]
0.20	0.98237	0.97872	0.97872
0.40	0.95524	0.95137	0.95137
0.60	0.90736	0.90312	0.90312
0.80	0.82935	0.82473	0.82473
0.90	0.76612	0.76168	0.76168
0.92	0.74879	0.74455	0.74454
0.94	0.72835	0.72451	0.72446
0.96	0.70285	0.69991	0.69968
0.98	0.66711	0.66705	0.66555

numerical results calculated by Tang [32] are also listed in Table 1. After comparing with those results in the literature, the present results are acceptable.

6.2. A circular bar containing an eccentric hole

For the second case, a circular bar containing an eccentric hole is considered as shown in Fig. 4(b). This case can be seen as a special case by setting $G_1 = 0$ in the first case. In this way, Eq. (87) can be reduced to

$$\begin{bmatrix} \mathrm{Re}[\mathbf{T}_{00}^m \overline{\mathbf{n}}_0^m] & \mathrm{Re}[\mathbf{T}_{01}^m \overline{\mathbf{n}}_1^m] & \mathrm{Re}(G_0\{\mathbf{p}_0^m\}) \\ \mathrm{Im}[\mathbf{T}_{00}^m \overline{\mathbf{n}}_0^m] & \mathrm{Im}[\mathbf{T}_{01}^m \overline{\mathbf{n}}_1^m] & \mathrm{Im}(G_0\{\mathbf{p}_0^m\}) \\ \mathrm{Re}[\mathbf{T}_{10}^m \overline{\mathbf{n}}_0^m] & \mathrm{Re}[\mathbf{T}_{11}^m \overline{\mathbf{n}}_1^m] & \mathrm{Re}(G_0\{\mathbf{p}_1^m\}) \\ \mathrm{Im}[\mathbf{T}_{10}^m \overline{\mathbf{n}}_0^m] & \mathrm{Im}[\mathbf{T}_{11}^m \overline{\mathbf{n}}_1^m] & \mathrm{Im}(G_0\{\mathbf{p}_1^m\}) \\ \{\mathbf{q}_0^m\}^T & \{\mathbf{q}_1^m\}^T & -G_0 I_{p_0} \\ \{\mathbf{l}_0^m\}^T & 0 & -2G_0 A_0 \\ 0 & \{\mathbf{l}_1^m\}^T & -2G_0 A_1 \end{bmatrix} \begin{Bmatrix} \boldsymbol{\beta}_0^m \\ \boldsymbol{\beta}_1^m \\ \alpha \end{Bmatrix} = \begin{Bmatrix} 0 \\ 0 \\ 0 \\ 0 \\ M \\ 0 \\ 0 \end{Bmatrix} \tag{97}$$

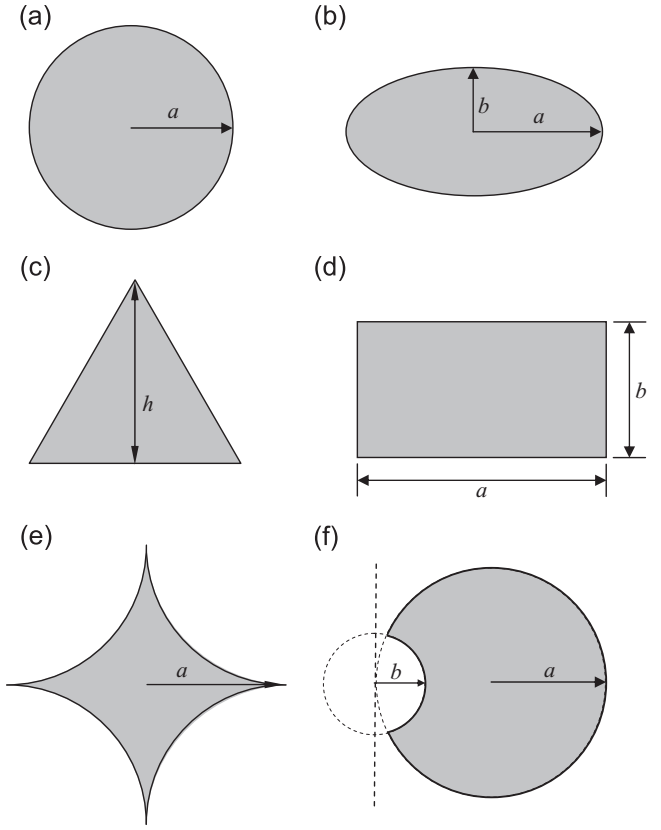

Fig. 5. Geometry of the cross-section. (a) Circle, (b) Ellipse, (c) Equilateral triangle, (d) Rectangle, (e) Astroid and (f) Circular cross section with a keyway

Table 3
Torsional rigidity of a circular bar versus the number of elements.

$a=1$	Present CVBEM	Analytical solution	Relative error (%)
$N=10$	1.58189	1.57080	0.706
$N=20$	1.62912		3.713
$N=30$	1.62123		3.211
$N=40$	1.61288		2.679
$N=50$	1.60649		2.272
$N=100$	1.59063		1.263
$N=150$	1.58445		0.869
$N=200$	1.58120		0.662
$N=250$	1.57920		0.535
$N=300$	1.57784		0.448

The dimensionless ratios of the torsional rigidity versus different case are shown in Table 2. The present results are compared with the exact solutions derived by Muskhelishvili [14] and semi-analytical solutions obtained from Chen et al. [33]. After comparison, the present results are acceptable.

6.3. A solid torsion bar

In this case, six kinds of solid torsion bars are considered. The sketches of cross sections are depicted in Fig. 5. On the basis of the present CVBIE, we have

$$\begin{bmatrix} \mathrm{Re}[\mathbf{T}_{00}^m \overline{\mathbf{n}}_0^m] & \mathrm{Re}(G_0\{\mathbf{p}_0^m\}) \\ \mathrm{Im}[\mathbf{T}_{00}^m \overline{\mathbf{n}}_0^m] & \mathrm{Im}(G_0\{\mathbf{p}_0^m\}) \\ \{\mathbf{q}_0^m\}^T & -G_0 I_{p_0} \\ \{\mathbf{l}_0^m\}^T & -2G_0 A_0 \end{bmatrix} \begin{Bmatrix} \boldsymbol{\beta}_0^m \\ \alpha \end{Bmatrix} = \begin{Bmatrix} 0 \\ 0 \\ M \\ 0 \end{Bmatrix}. \tag{98}$$

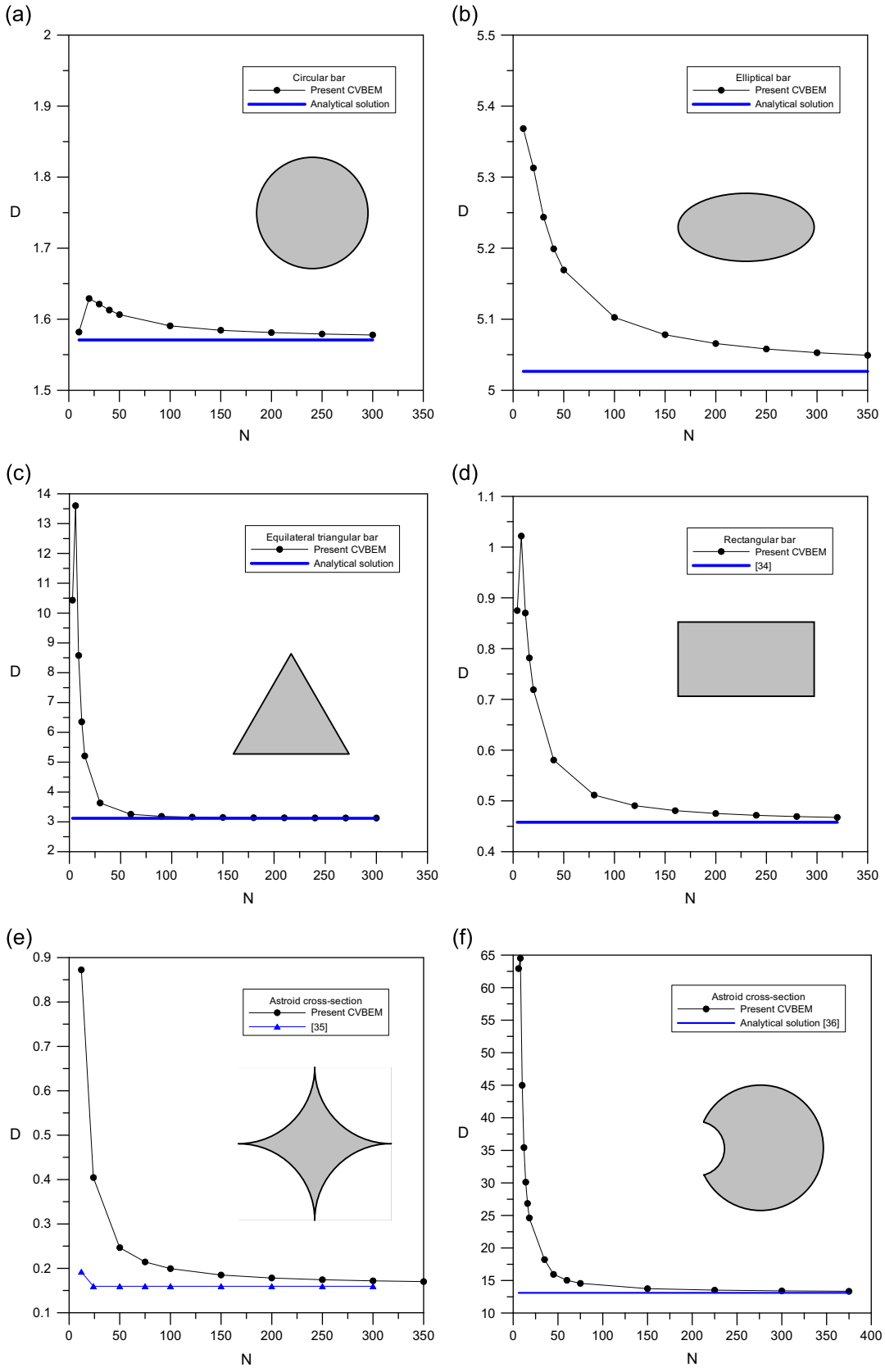

Fig. 6. Sketches of the torsional rigidity versus the number of elements. (a) Circular bar, (b) Elliptical bar (c) Equilateral triangular bar (d) Rectangular bar (e) Bar with astroid cross-section and (f) Circular cross section with a keyway

For the circular case with a radius ($a = 1$) as shown in Fig. 5(a), numerical results for the torsional rigidity versus the number of elements are listed in Table 3. Also, the convergence curve is plotted in Fig. 6(a). However, the rate of convergence is not fast. After comparing with the analytical solution, the numerical results obtained by the present CVBEM are acceptable. In the conventional boundary

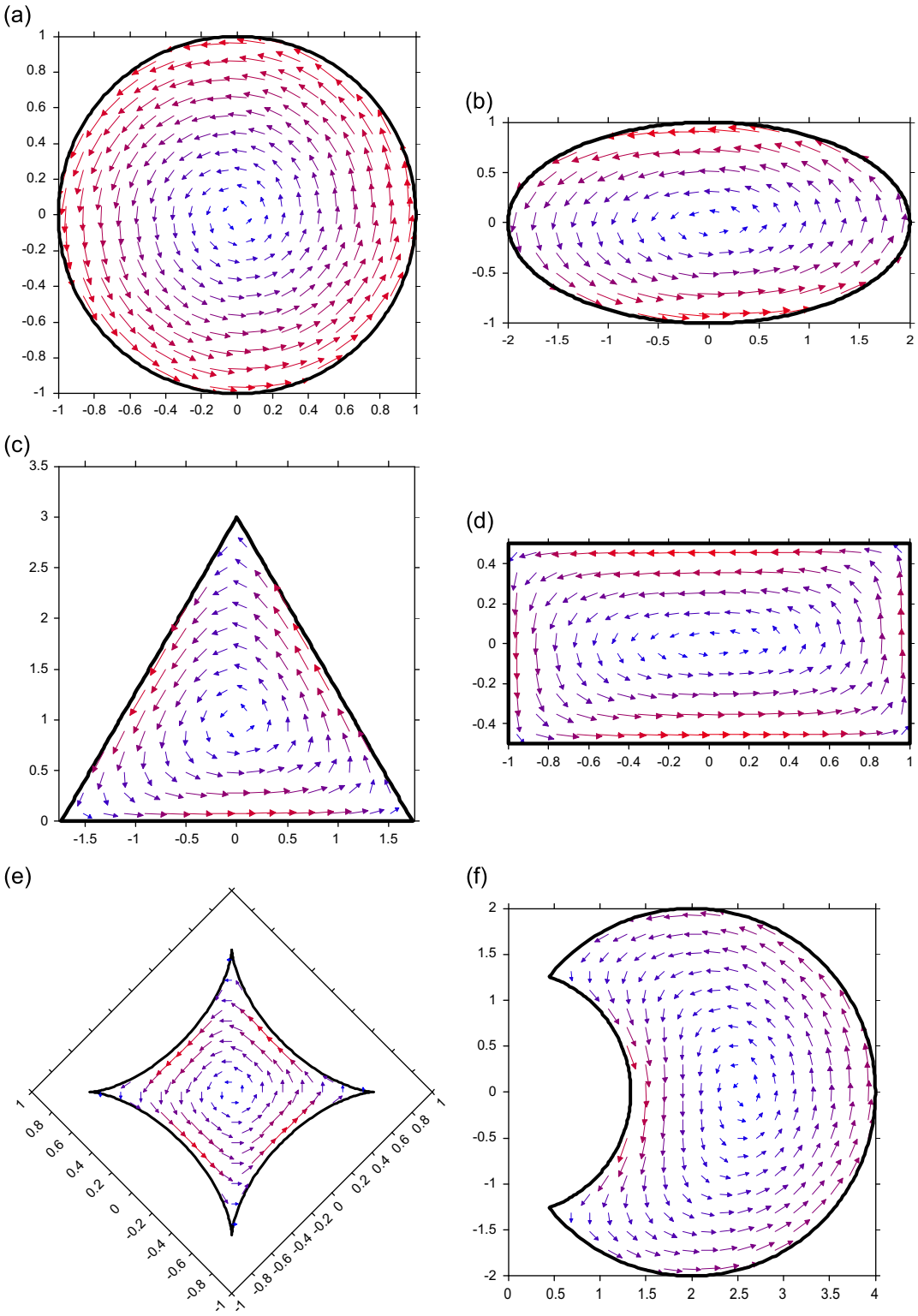

Fig. 7. Vector field of the two shear stress fields. (a) Circular bar, (b) Elliptical bar, (c) Equilateral triangular bar, (d) Rectangular bar, (e) Bar with astroid cross-section, and (f) Circular cross section with a keyway

integral formulations, only the normal derivative is required and the tangent derivative is not. While the differential term in the present CVBIE contains both normal and tangent derivatives along the boundary. In our real implementation, the constant element scheme is employed. The rate of convergence is not fast due to need of more constant elements to simulate the tangent derivative. This can explain why lower number of element cannot yield good results. Nevertheless, the present CVBIE still has its benefits for solving the torsion problems. Not only the torsional rigidity but also the stress fields can be straightforward obtained. The stress flow of a circular bar subjected to a torque is plotted in Fig. 7(a). For the other cases as shown in Fig. 5(b)–(f), the torsional rigidities versus the number of elements are

Table 4
Torsional rigidity of an elliptical bar versus the number of elements.

$a=2,\ b=1$	Present CVBEM	Analytical solution	Relative error (%)
$N=10$	5.36838	5.02655	6.800
$N=20$	5.31295		5.698
$N=30$	5.24362		4.319
$N=40$	5.19911		3.433
$N=50$	5.16925		2.839
$N=100$	5.10251		1.511
$N=150$	5.07821		1.028
$N=200$	5.06567		0.778
$N=250$	5.05803		0.626
$N=300$	5.05288		0.524
$N=350$	5.04918		0.450

Table 5
Torsional rigidity of an equilateral triangular bar versus the number of elements.

$h=3$	Present CVBEM	Analytical solution	Relative error (%)
$N=3$	10.43335	3.11769	234.650
$N=6$	13.60130		336.262
$N=9$	8.57845		175.154
$N=12$	6.35489		103.833
$N=15$	5.20880		67.072
$N=30$	3.63319		16.535
$N=60$	3.25438		4.384
$N=90$	3.18463		2.147
$N=120$	3.15925		1.333
$N=150$	3.14690		0.937
$N=180$	3.13981		0.710
$N=210$	3.13531		0.565
$N=240$	3.13223		0.466
$N=270$	3.13001		0.395
$N=300$	3.12834		0.341

Table 6
Torsional rigidity of a rectangular bar versus the number of elements.

$a=2,\ b=1$	Present CVBEM	[34]	Relative error (%)
$N=4$	0.875	0.458	91.032
$N=8$	1.022		123.088
$N=12$	0.870		89.974
$N=16$	0.782		70.667
$N=20$	0.719		57.006
$N=40$	0.580		26.727
$N=80$	0.512		11.682
$N=120$	0.490		7.093
$N=160$	0.481		4.959
$N=200$	0.475		3.748
$N=240$	0.472		2.978
$N=280$	0.469		2.448
$N=320$	0.467		2.064

Table 7
Torsional rigidity of a bar with astroid cross-section versus the number of elements.

$a=1,\ m=4$	Present CVBEM	CPM [35]	Relative error (%)
$N=12$	0.87235	0.19209	354.136
$N=24$	0.40443	0.15965	153.325
$N=50$	0.24658	0.15960	54.502
$N=75$	0.21438	0.15960	34.326
$N=100$	0.19934	0.15960	24.899
$N=150$	0.18492	0.15960	15.863
$N=200$	0.17831	0.15960	11.721
$N=250$	0.17436	0.15960	9.248
$N=300$	0.17182	0.15960	7.660
$N=350$	0.17001	N.A.	N.A.

Table 8
Torsional rigidity of a circular bar with a keyway versus the number of elements.

$a=2,\ b=\frac{2}{3}a$	Present CVBEM	Analytical solution [36]	Relative error (%)
$N=6$	62.93100	13.09329	380.636
$N=8$	64.52612		392.818
$N=10$	44.99025		243.613
$N=12$	35.42487		170.557
$N=14$	30.10976		129.963
$N=16$	26.83087		104.921
$N=18$	24.60360		87.910
$N=30$	18.20703		39.056
$N=45$	15.93643		21.714
$N=60$	15.02877		14.782
$N=75$	14.55172		11.139
$N=150$	13.73927		4.934
$N=225$	13.50720		3.161
$N=300$	13.39773		2.325
$N=375$	13.33403		1.839

given in Tables 3–8. For these five cases, our numerical results are also acceptable after comparing with those in literature [34–36]. Also the figures of the convergence curve are plotted in Fig. 6(b)–(f) and Fig. 7(b)–(f) showing the vector field of the stress flow.

7. Conclusions

In this paper, we have successfully proposed a new complex variable boundary integral equation (CVBIE) based on the general Cauchy integral formula to solve the Saint-Venant's torsion problems in stress variables. The general Cauchy integral formula has been derived from the Borel–Pompeiu formula. Different from the conventional CVBIE based on the Cauchy integral formula, the present one not only can solve for holomorphic (analytic) functions but also for complex-valued harmonic functions. The main character of the present method is that we can directly solve the two shear stress fields at the same time. By using the present approach for solving the Saint-Venant's torsion problems, two benefits can be gained. The stress fields and the torsional rigidity can be directly determined without any numerical differentiation and integration again, respectively. Also, the torsional rigidity can be obtained at once. From the above view point, the present CVBIE is more general and convenient than the conventional one when solving the Saint-Venant's torsion problems.

References

[1] Barone MR, Caulk DA. Optimal arrangement of holes in a two-dimensional heat conductor by a special boundary integral method. Int J Numer Methods Eng 1982;18:675–85.
[2] Cheng HW, Greengard L. On the numerical evaluation of electrostatic field in dense random dispersions of cylinders. J Comput Phys 1997;136:629–39.
[3] Caulk DA. Analysis of elastic torsion in a bar with circular holes by a special boundary integral method. J Appl Mech Trans ASME 1983;50:101–8.
[4] Chen JT, Hong H-K, Chyuan SW. Boundary element analysis and design in seepage problems using dual integral formulations. Finite Elem Anal Des 1994;17(1):1–20.
[5] Hutchinson JR. An alternative BEM formulation applied to membrane vibrations. In: Brebbia CA, Maier G, editors. Boundary elements VII. Berlin: Springer-Verlag; 1985.
[6] Chen KH, Chen JT, Chou CR, Yueh CY. Dual boundary element analysis of oblique incident wave passing a thin submerged breakwater. Eng Anal Bound Elem 2002;26:917–28.
[7] Chen JT, Chen KH. Dual integral formulation for determining the acoustic modes of a two-dimensional cavity with a degenerate boundary. Eng Anal Bound Elem 1998;21(2):105–16.
[8] García-Castillo LE, Gómez-Revuelto I, Sáez de Adana F, Salazar-Palma M. A finite element method for the analysis of radiation and scattering of electromagnetic waves on complex environments. Comput Methods Appl Mech Eng 2005;194:637–55.

[9] Chen JT, Chen PY, Chen CT. Surface motion of multiple alluvial valleys for incident plane SH-waves by using a semi-analytical approach. Soil Dyn Earthq Eng 2008;28:58–72.
[10] Mills RD. Computing internal viscous flow problems for the circle by integral methods. J Fluid Mech 1977;73:609–24.
[11] Hutchinson JR. Vibration of plates. In: Brebbia CA, editor. Boundary elements X. Berlin: Springer-Verlag; 1988.
[12] Brebbia CA. Boundary element methods. Berlin: Springer-Verlag; 1981.
[13] Chen JT, Hong H-K. Boundary element method. Taipei: New World Press; 1992 (in Chinese).
[14] Muskhelishvil NI. Some basic problems of the mathematical theory of elasticity. New York: Springer; 1953.
[15] Muskhelishvil NI. Singular Integral Equations. Dover, New York: Translated by Radok JRM; 1992.
[16] Hromadka II TV. Linking the complex variable boundary element method to the analytic function method. Numer Heat Transf 1984;7:235–40.
[17] Whitley RJ, Hromadka II TV. Complex logarithms, Cauchy principal values, and the complex variable boundary element method. Appl Math Model 1994;18:423–8.
[18] Whitley RJ, Hromadaka II TV. Theoretical developments in the complex variable boundary element method. Eng Anal Bound Elem 2006;30:1020–4.
[19] Chou SI, Shamas-Ahmadi M. Complex variable boundary element method for torsion of hollow shafts. Nucl Eng Des 1992;136:255–63.
[20] Linkov AM. Boundary integral equations in elasticity theory. Dordrecht: Springer; 2002.
[21] Gu L, Huang MK. A complex variable boundary element method for solving plane and plate problems of elasticity. Eng Anal Bound Elem 1991;8 (6):266–72.
[22] Kolhe R, Ye W, Hui CY, Mukherjee S. Complex variable functions for usual and hypersingular integral equations for potential problems with applications to corners and cracks. Comput Mech 1996;17:279–86.
[23] Chen JT, Chen YW. Dual boundary element analysis using complex variables for potential problems with or without a degenerate boundary. Eng Anal Bound Elem 2000;24(1):671–84.
[24] Di Paola M, Pirrotta A, Santoro R. Line element-less method (LEM) for beam torsion solution (truly no-mesh method). Acta Mech 2008;195:349–63.
[25] Barone G, Pirrotta A. CVBEM application to a novel potential function providing stress field and twist rotation at once. J. Eng. Mech.-ASCE 2013;139:1290–3.
[26] Hromadka II TV, Guymon LG. Complex polynomial approximation of the Laplace equation. J Hydraul Eng 1984;110:329–39.
[27] Pirrotta A. Complex potential function in elasticity theory: shear and torsion solution through line integrals. Acta Mech 2012;223(6):1251–9.
[28] Barone G, Pirrotta A. CVBEM for solving De Saint-Venant solid under shear forces. Eng Anal Bound Elem 2013;37:197–204.
[29] Pompeiu D. Sur une classe de fonctions d'une variable complexe et sur certaines équations intégrales. Rend Circ Mat Palermo 1913;35:277–81.
[30] Begehr H. Boundary value problems in complex analysis I. Bol Asoc Math Venez 2005;12:65–85.
[31] Chen JT, Lee YT. Torsional rigidity of a circular bar with multiple circular inclusions using the null-field integral approach. Comput Mech 2009;44:221–32.
[32] Tang RJ. Torsion theory of the crack cylinder. Shanghai: Shanghai Jiao Tong University Publisher; 1996 (in Chinese).
[33] Chen JT, Shen WC, Chen PY. Analysis of circular torsion bar with circular holes using null-field approach. CMES-Comput Model Eng Sci 2006;12(2):109–19.
[34] Timoshenko S, Goodier JN. Theory of elasticity. Third Ed. New York: McGraw Hill; 1970.
[35] Aleynikov SM, Stromov AV. Comparison of complex methods for numerical solutions of boundary problems of the Laplace equation. Eng Anal Bound Elem 2004;28:16.
[36] Reismann H, Pawlik PS. Elasticity theory and applications. New York: Wiley; 1980.